

Low-cost fiber-optic waveguide sensor for the colorimetric detection of ammonia

Katrin Schmitt^{*a}, Jonas Rist^a, Carolin Peter^a, Jürgen Wöllenstein^{a,b}

^aFraunhofer Institute for Physical Measurement Techniques, Heidenhofstr. 8, 79110 Freiburg, Germany

^bDepartment of Microsystems Engineering – IMTEK, University of Freiburg, Georges-Koehler-Allee 102, 79110 Freiburg, Germany

ABSTRACT

We present the development and characterization of a low-cost fiber-optic colorimetric gas sensor for ammonia combined with the electronic circuitry for measurement control and RFID communication. The gas sensor detects ammonia using a 300 μm polyolefin fiber coated with a gas-sensitive polymer film. The spectral and time-dependent sensitivity of various polymer films was tested in transmission measurements at $\lambda = 590\text{ nm}$. A prototype of the gas sensor was tested under realistic measurement conditions, i.e. battery-driven and in a completely autonomous mode. The sensor system showed good sensitivity to the ammonia concentrations and response times in the order of minutes. The achievable power consumption was below $100\mu\text{W}$. Bromophenol blue-based films showed a strong reaction to ammonia, with saturation concentrations around 1000 ppm and response times of about 15 seconds to 100ppm. The colorimetric reaction was simulated using a simple kinetic model which was in good agreement with the experimental results.

Keywords: fiber optical waveguide, ammonia detection, colorimetric, RFID

1. INTRODUCTION

In recent years a rising need for ammonia sensors could be observed. Applications fields of ammonia sensors include environmental monitoring, biomedicine, process monitoring and the control of perishable goods (Rogers and Poziomek 1996; Wolfbeis 1990; Pacquit et al. 2004). The sensors do not need a high accuracy, but a compact setup, long-term stability, low energy consumption and low fabrication costs, and optionally wireless data communication. Low-cost sensors combined with wireless data communication offer the possibility to establish sensor networks, e.g. distributed in food storages or containers. Among the important gases to monitor are oxygen (O’Keeffe 1995), CO_2 (Mills 1992), and ammonia (NH_3) (Timmer 2005). Depending on the application, required concentrations for NH_3 detection are between 50 ppb and 1000 ppm. NH_3 monitoring is of high relevance for example in pig sties and their vicinity, breath analysis, leakage detection in chemical plants, or the selective catalytic reduction of NO_x in exhaust gases using ammonia. Due to the multitude of applications, NH_3 was chosen as the target gas for the proposed colorimetric fiber waveguide sensor.

Already in 1975, Hardy et al. analyzed the chemical reactions in a polymer-coated waveguide in transmission (Hardy et al. 1975). One year later, David et al. (1976) coated a cylindrical quartz rod with a layer consisting of polyvinylpyrrolidone and ninhydrin (2,2-dihydroxyindane-1,3-dione). They achieved detection limits in the ppb range for gaseous NH_3 , yet the reaction is irreversible. In 1983, Guiliani et al. used a capillary as optical waveguide with a pH-sensitive oxazine-perchlorate layer, for the reversible detection of 60 to 1000 ppm NH_3 (Guiliani et al. 1983). As a result, several substances were implemented in colorimetric sensors; most of them are pH-sensitive and react to the alkalinity of NH_3 (Mills 1995; Brandenburg et al. 1995). Often used is the pH-indicator dye bromophenol blue (Courbat et al. 2009/1 and Courbat et al. 2009/2). Due to its high sensitivity to NH_3 and easy handling, we used this dye throughout the experiments described in this paper. Our aim was to combine the optical readout of colorimetric indicator layers on fibers with wireless data communication to obtain a sensor suitable for use in demanding environments.

*katrin.schmitt@ipm.fraunhofer.de; phone 49 761 8857-316; fax 49 761 8857-224; www.ipm.fraunhofer.de

2. SENSOR PRINCIPLE

The optical readout of colorimetric layers is an interesting approach in the development of gas sensors with the above mentioned features. Fig. 1 shows schematically the measurement principle. An optical waveguide, planar or fiber, is illuminated by a suitable light source (e.g. LED). On the opposite side, the transmitted intensity is detected by a photodiode (PD). The waveguide is coated with a sensitive layer consisting of the colorimetric dye embedded in a polymer matrix. Upon exposure to the target gas, in our case NH_3 , the colorimetric dye changes its color, leading to a change in absorption and thus the transmitted light intensity. This approach is advantageous for several reasons: the broad absorption and absorption changes of the colorimetric dye allow the use of a low-cost LED; furthermore, the power consumption of LED and PD are very low compared to other sensing techniques and allow an autonomous operation of the gas sensor.

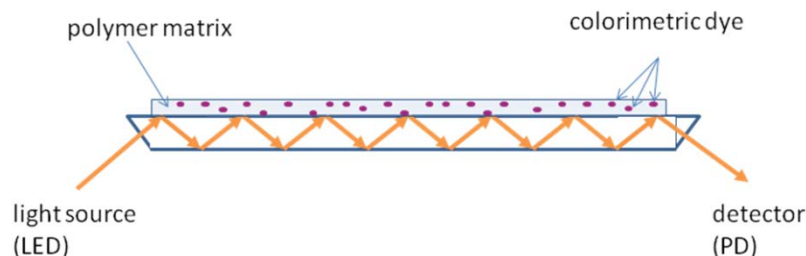


Figure 1. Principle of a colorimetric gas sensor: ambient gas (e.g. NH_3) changes the color and thus absorption of the sensitive layer consisting of the colorimetric dye embedded in a polymer matrix. The sensitive layer is coated on an optical waveguide (planar or fiber), illuminated by light from a suitable light source (e.g. LED). The change in absorption can be detected by a change in the light intensity on the detector (e.g. photodiode).

3. EXPERIMENTAL

3.1 RFID communication

The electronic circuitry of the gas sensor controls the measurements and allows communication with a PC, both with the lowest possible power consumption. For RFID communication, a commercially available RFID reader (Scemtec, Germany) was used and the corresponding transponder developed and integrated on the gas sensor system, based on high-frequency RFID according to ISO 15693. Fig. 2a depicts the components of the RFID system with reader, reader antenna and transponder, Fig. 2b gives the setup of the electronic circuitry. The key component of the electronics is the microcontroller (PSoc, Cypress). For the implementation of the RFID protocol an adapted circuitry was used between the microcontroller and the SPI interface. The microcontroller also triggers and reads the LED and PD, thereby measuring the present gas concentration.

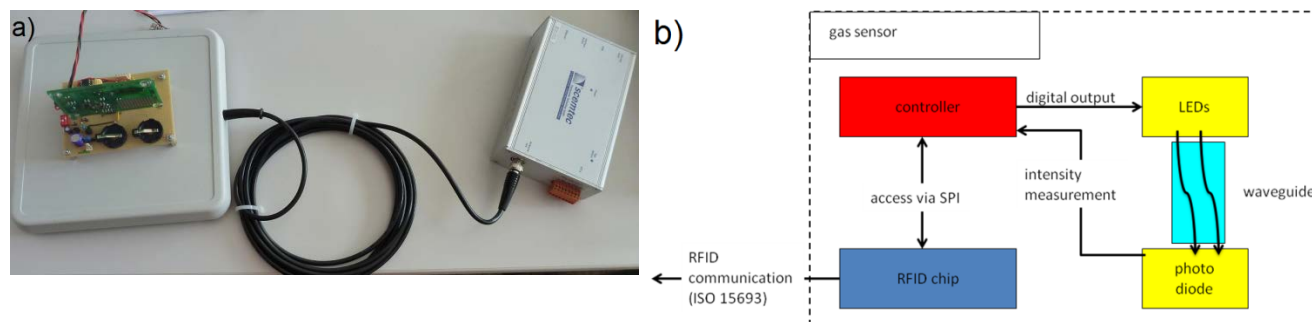


Figure 2. a) Photograph of the RFID system with reader (right), reader antenna (left) and transponder (on top)
b) Setup of the electronic circuitry: the key component is the microcontroller, controlling the LED and reading the photodiode. The same controller communicates with the PC via the RFID chip.

To date, only a few integrated (packaged) circuitries are freely available for RFID protocol implementation. One of them is the Melexis MLX90129, which can be controlled via an SPI interface, and comes with a 4096bit internal EEPROM (Electrically Erasable Programmable Read-Only Memory), which can be accessed either via SPI or via RFID. The data transfer between PC and microcontroller is accomplished using the EEPROM. The chip also contains a high-frequency module for radio transmission. As external circuitry only a suitable antenna is needed, this can be integrated as conductor line on the circuit board.

3.2 Transmission measurements

Polyolefin optical fibers (Paradigm Optics, USA) with 300 μm diameter were characterized regarding their attenuation and coupling efficiency depending on different optical setups. To estimate coupling efficiency, standard LEDs at 590 nm in comparison to 630 nm were used, and direct front face coupling compared with the use of an aspheric lens with a focal length of 8 mm. For the determination of attenuation, the fibers were successively cut at one end and the remaining transmission measured, under the assumption of a constant attenuation along the fiber. Describing the measured data with an exponential fit, the attenuation coefficient could be determined. The total optical power of the LEDs was previously measured with an optical power meter (1936C, Newport, USA), as detector a simple photodiode (S1133, Hamamatsu, Japan) was used. The photodiode has a relatively large active area of $\sim 8\text{mm}^2$, so that we could assume to record the complete optical power emitted at the fiber end. Furthermore, the combination of an aspheric lens ($f = 8\text{ mm}$) with an uncollimated LED or a LED collimated with a microscope objective was investigated. In all cases the light was focused on the front face of the fiber.

3.3 Fabrication of NH_3 -sensitive layers

For the sensitive layers, the pH indicator dye bromophenol blue (BPB) (AppliChem, Germany) was dissolved in 99.9% ethanol (Roth, Germany) and mixed with either ethyl cellulose (EC) or polyvinyl butyral (PVB), both obtained from Sigma-Aldrich, Germany, also dissolved in 99.9% ethanol. Optionally tributylphosphate (Fluka, Germany) was added as plasticizer. Table 1 gives the composition of the sensitive layers.

Table 1. Composition of the colorimetric layers

| # | composition |
|---|--|
| 1 | 1g EC + 33.3mg BPB + 22.6ml ethanol |
| 2 | 1g EC + 33.3mg BPB + 22.6ml ethanol + 1ml TBP |
| 3 | 1g PVB + 33.3mg BPB + 22.6ml ethanol + 1ml TBP |

3.4 UV/VIS spectroscopic measurements and film characterization

UV/VIS spectroscopic measurements were performed in transmission using glass windows suitable for the Lambda 900 UV/VIS spectrometer (Perkin Elmer, USA). The glass windows were used to obtain the absorption spectra of the different compositions of sensitive layers, which is much easier as in the waveguide configuration. The windows were coated either through spin-coating or dip-coating. All sensitive layers were characterized with a profilometer (Dektak 6M) after locally wiping off the layer. By this, a blurred edge is produced across which the layer thickness can be determined and the roughness calculated from the scanned profile.

4. RESULTS AND DISCUSSION

4.1 Transmission measurements

The transmission measurements should give information about the attenuation of the polyolefin fiber, and the coupling efficiencies of different optical setups. For each measurement the coupling setup was aligned and optimized once. The results show that direct front face coupling is easier to miniaturize, stable and does not require elaborated alignment. However, the reproducibility obtained was poor, and the coupling efficiency was around 0.1% of that obtained with the aspheric lens. The LED additionally collimated with the microscope objective showed a lower coupling efficiency, since the collimated beam had a larger diameter than the aspheric lens and therefore a large fraction of the light power was lost.

The collimated LED resulted in a lower efficiency due to a higher beam cross section and thus loss of total optical power. Fig. 3 compares the transmission powers for two LEDs at 590 nm and 630 nm, and direct front face and collimated coupling. The results show that after normalization the transmitted power remains almost identical for all coupling methods. Therefore we chose to use direct front face coupling for the sensor setup due to the easier adjustment and integration. Table 2 summarizes the results. For the setup of the prototype gas sensor we chose direct front face coupling due to the easy integration.

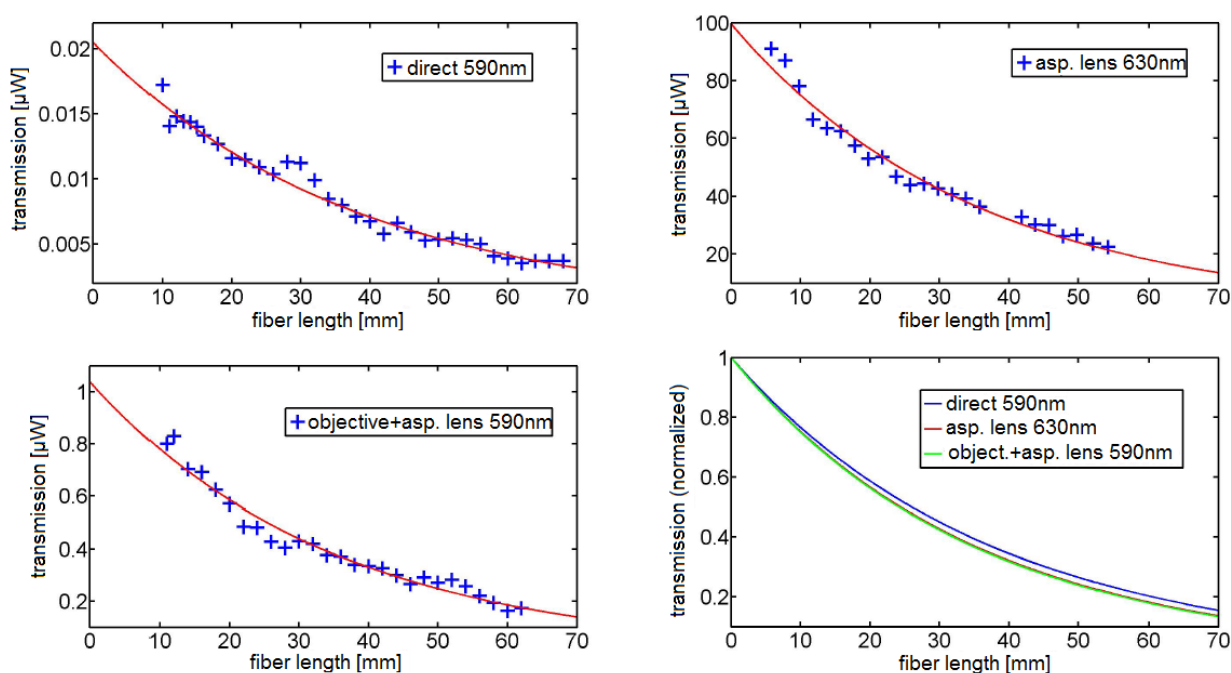


Figure 3. Comparison of the total transmitted optical power through a 300 μm polyolefin fiber, using direct front face coupling (upper left), collimated with an aspheric lens at 630 nm (upper right), collimated using a microscope objective and the aspheric lens at 590 nm (lower left) and the normalized comparison (lower right), depending on the fiber length. It can be seen that for each coupling method the normalized transmitted power remains almost identical.

Table 2. Parameters and results of the transmission measurements: λ : wavelength of LEDs, P_0 : LED intensity, P_{in} : incoupled light intensity (from exponential curve), η : coupling efficiency, α : damping coefficient

| λ [nm] | P_0 [mW] | P_{in} [μW] | η [%] | α [m^{-1}] | coupling method |
|----------------|------------|----------------------------|------------|------------------------------|-------------------|
| 590 | 1.8 | 0.02 | 0.001 | 0.266 | direct front face |

| | | | | | |
|-----|-----|------|------|-------|-------------------------------------|
| 590 | 2.2 | 1.0 | 0.05 | 0.287 | objective + aspheric lens (f = 8mm) |
| 630 | 6.7 | 99.6 | 1.5 | 0.284 | aspheric lens (f = 8mm) |

4.2 UV/VIS spectroscopic measurements and film characterization

Fig. 4 shows photographs comparing spin-coated and dip-coated layers. The difference in the topography is clearly visible: with dip-coating a significantly smoother surface could be obtained with $\sim 1/10$ of the roughness of the spin-coated layers.

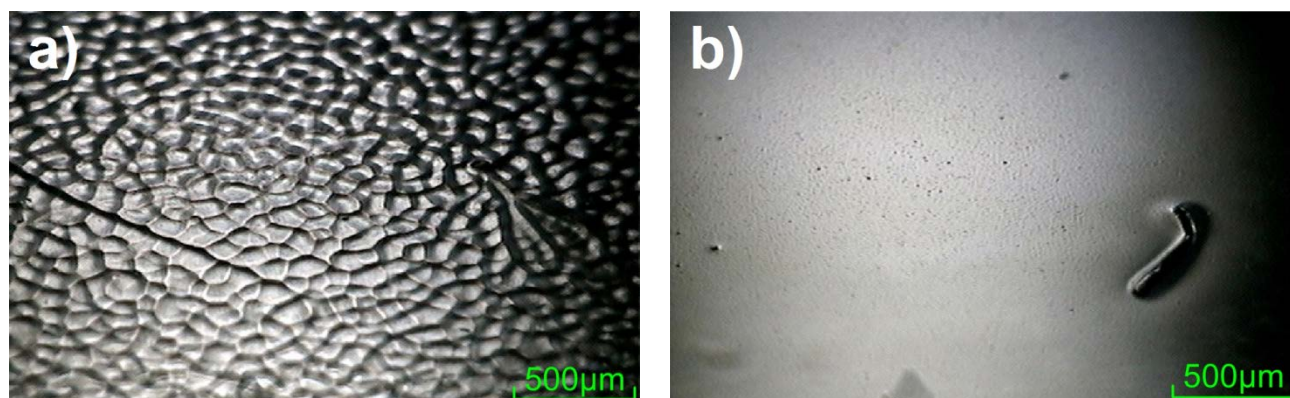
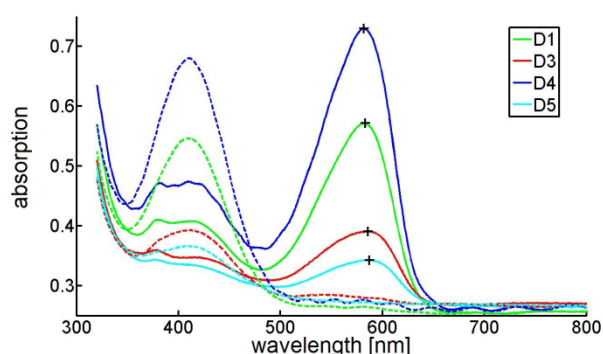


Figure 4. Photographs of polymeric layers on glass, a) spin-coated b) dip-coated. Clearly visible is the difference in topography. Spin-coating results in surfaces with ~ 10 -fold higher roughness than spin-coating.

To derive the optimal operation wavelength of the LED in the gas sensor system, the absorption of the colorimetric layers obtained from compositions 1-3 (cf. Table 1) was compared using the UV/VIS spectrometer in transmission configuration. All samples were mounted in a gas tight cuvette for the NH_3 measurements. Mass-flow controllers are used to control the composition and gas flow. The highest NH_3 concentration was 1000 ppm at a gas flow of 0.1 l/min. N_2 was used as carrier gas. Fig. 5 shows the absorption spectra of BPB in exposed to pure N_2 and 100 ppm NH_3 . The absorption maxima at ~ 600 nm show a hypsochromic shift for layers with higher sensitivity. This can be attributed to the higher layer thickness. For layers with thicknesses between $0.4 \mu\text{m}$ and $2.2 \mu\text{m}$, the shift is < 5 nm. The table gives the correlation between dip velocity and layer thickness. Layers coated at higher dip velocities have a higher thickness.



| Sample | Dip velocity [$\mu\text{m/s}$] | Layer thickness [μm] | Roughness [nm^2] |
|--------|----------------------------------|-----------------------------------|-----------------------------|
| D1 | 500 | 1.5 | 16 |
| D3 | 100 | 0.6 | 38 |
| D4 | 1000 | 2.2 | 31 |
| D5 | 30 | 0.4 | 28 |

Figure 5. Absorption spectra of BPB in exposed to pure N_2 (dashed lines) and 100 ppm NH_3 (solid lines). The absorption maxima at ~ 600 nm show a hypsochromic shift for layers with higher sensitivity, i.e. higher layer thickness. For layers with thicknesses between $0.4 \mu\text{m}$ and $2.2 \mu\text{m}$, the shift is < 5 nm. The table gives the correlation between dip velocity and layer thickness. Layers coated at higher dip velocities have a higher thickness.

Fig. 6 shows the results from the comparison between samples containing TBP or without TBP upon exposure to 100 ppm NH_3 . While the absolute transmission is higher for the sample without TBP, the sample containing TBP shows a higher relative absorption for the same gas concentration. For this reason, we continued with colorimetric layers containing TBP for further experiments with fibers. It can further be deduced that an LED operating at 590 nm is optimal for integration in the sensor system.

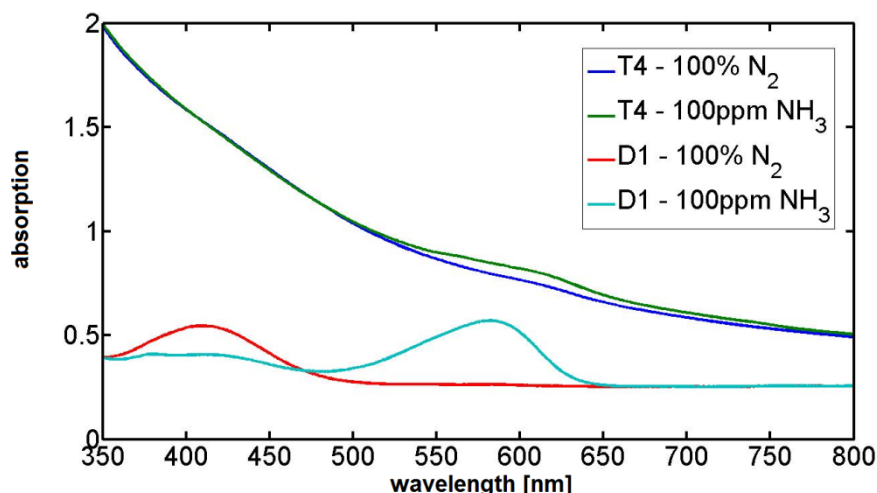


Figure 6. Comparison of transmission spectra of two samples with (D1) and without (T4) TBP. Both samples show increased absorption at ~ 600 nm upon exposure to 100 ppm NH_3 . While the absolute transmission is higher for the sample without TBP, the sample containing TBP shows a higher relative absorption for the same gas concentration.

In the next step, a concentration series from 10 ppm to 100 ppm NH_3 was measured (data not shown). The sensor responses for each concentration was taken from the sensorgrams and plotted against the respective concentration. These data points were fitted to the Langmuir model to obtain the absorption coefficients of the different compositions. As an example, Fig. 7 shows the results for composition 3, yielding an absorption coefficient of $0.25/\mu\text{m}$.

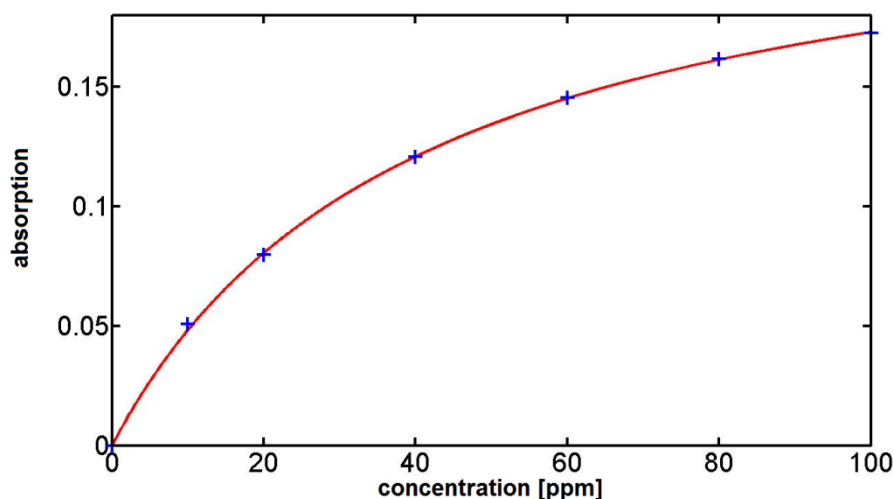


Figure 7. Sensitivity of sample with composition 3 (cf Table 1) for different concentrations of NH_3 . The data points can be fitted to the kinetic model derived by Langmuir to obtain an absorption coefficient of $0.25/\mu\text{m}$.

4.3 Fiber-optic sensor characterization

For a test of a prototype gas sensor system including RFID communication and a fiber coated using composition 3, it was placed into a small measurement chamber and exposed to NH_3 concentrations ranging from 10 ppm to 1000 ppm. The sensor was operated autonomously, i.e. battery driven. Fig. 8 shows a photograph of the prototype gas sensor and the resulting sensorgram of the NH_3 measurement. The sensor responds to all concentrations, with response times between four and ten minutes depending on the concentration. The high response times were probably due to the lack of a flow cell, so that the NH_3 required several minutes to fill the measurement chamber. The detection limit of this sensor can be estimated to 5 ppm.

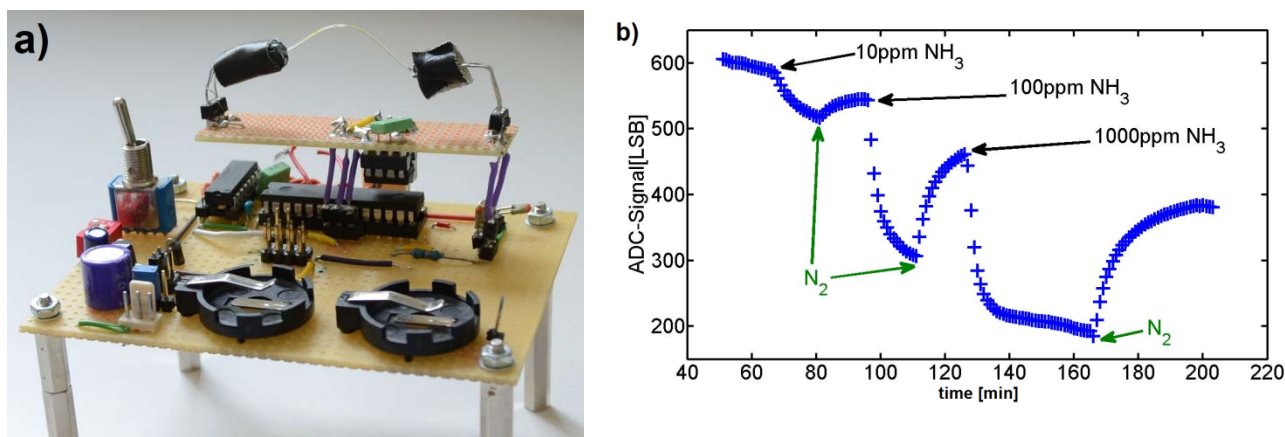


Figure 8. a) Photograph of the prototype gas sensor, b) sensorgram of the fiber optical sensor using composition 3 upon exposure with 10, 100 and 1000 ppm NH_3 . The sensor response times were several minutes. The detection limit of this sensor can be estimated to 5 ppm.

5. CONCLUSIONS AND OUTLOOK

In this paper we have shown the development of an optical fiber waveguide sensor implementing colorimetric sensitive layers for the detection of NH_3 . The sensor is combined with an electronic circuitry for measurement control and wireless communication, which was successfully tested by a bidirectional communication test between the microcontroller and the corresponding RFID reader connected to a PC. The sensor was operated in a completely autonomous mode, i.e. battery driven, and the stored measurement results could be read via RFID. The power consumption of the device was around $860\mu\text{W}$.

For the assessment of the sensitivity and stability of the colorimetric layers, different polymers were tested with the pH indicator dye bromophenol blue. These layers were characterized both in transmission using an UV/VIS spectrophotometer, and on $300\mu\text{m}$ polyolefin fibers in waveguide configuration. The stability of the layers could be enhanced using tributylphosphate as plasticizer. The bromophenol blue-containing films showed a strong reaction to NH_3 , with saturation concentrations around 1000 ppm, and response times of several minutes. The chemical reaction was simulated using the Langmuir model. The experimental results obtained for most of the films were in good agreement with this model. Yet the sensitivity and kinetic rate constants decreased within a few days after preparation. The next steps will include the improvement of the long-term stability of the films as well as their modification towards other target gases. In addition software improvements will further reduce the required power.

ACKNOWLEDGEMENTS

We acknowledge financial support from the European Community in the framework of the Eurostars Programme and Rhenovia Pharma.

REFERENCES

- Brandenburg A, Edelhäuser R, Werner T, He H, Wolfbeis OS (1995) Ammonia detection via integrated optical evanescent wave sensors. *Mikrochim. Acta* 121: 95-105
- Courbat J, Briand D, Damon-Lacoste J, Wöllenstein J, de Rooij NF (2009) Evaluation of pH indicator-based colorimetric films for ammonia detection using optical waveguides. *Sens Actuators B* 143: 62-70
- Courbat J, Briand D, Wöllenstein J, de Rooij NF (2009) Colorimetric gas sensors based on optical waveguides made on plastic foil. *Procedia Chemistry* 1: 576-579
- David DJ, Willson MC, Ruffin OS (1976). Direct measurement of ammonia in ambient air. *Anal Lett* 9(4): 389-404
- Guiliani JF, Wohltjen H, Jarvis NL (1983). Reversible optical waveguide sensor for ammonia vapors. *Opt Lett* 8: 54-56
- Hardy EE, David DJ, Kapany NS, Unterleitner FC (1975). Coated optical guides for spectrophotometry of chemical reactions. *Nature* 257: 666-667
- Mills A, Chang Q, McMurray N (1992) Equilibrium studies on colorimetric plastic film sensors for carbon dioxide. *Anal Chem* 64: 1383-1389
- Mills A, Wild L, Chang Q (1995) Plastic colorimetric film sensors for gaseous ammonia. *Mikrochim Acta* 121: 225-236
- O'Keeffe G, MacCraith BD, McEvoy AK, McDonagh MC, McGilp JF (1995) Development of a LED-based phase fluorimetric oxygen sensor using evanescent wave excitation of a sol-gel immobilized dye. *Sens Actuators B* 29: 226-230
- Pacquit A, Lau KT, Diamond (2004) Development of a colorimetric sensor for monitoring of fish spoilage amines in packaging headspace. *Proc IEEE* 1: 665-667
- Rogers KR, Poziomek EJ (1996) Fiber optic sensor for environmental monitoring. *Chemosphere* 33(6): 1151-1174
- Timmer B, Olthius W, van den Berg A (2005) Ammonia sensors and their applications – a review. *Sens Actuators B* 107: 666-677
- Wolfbeis OS (1990) Chemical sensors – survey and trends. *Fresenius J Anal Chem* 337: 522-527